

INTRINSIC CHARM AND $D^+ - D^-$ ASYMMETRY IN PP COLLISIONS



Gennady Lykasov¹

in collaboration with
Stanley Brodsky²
and

Maxim Sorokovikov¹

¹JINR, Dubna,

*²SLAC, Stanford University,
United States*

**G.L., M.N. Sorokovikov, S.J., Brodsky,
Phys.Rev. D111, 074035 (2025)**

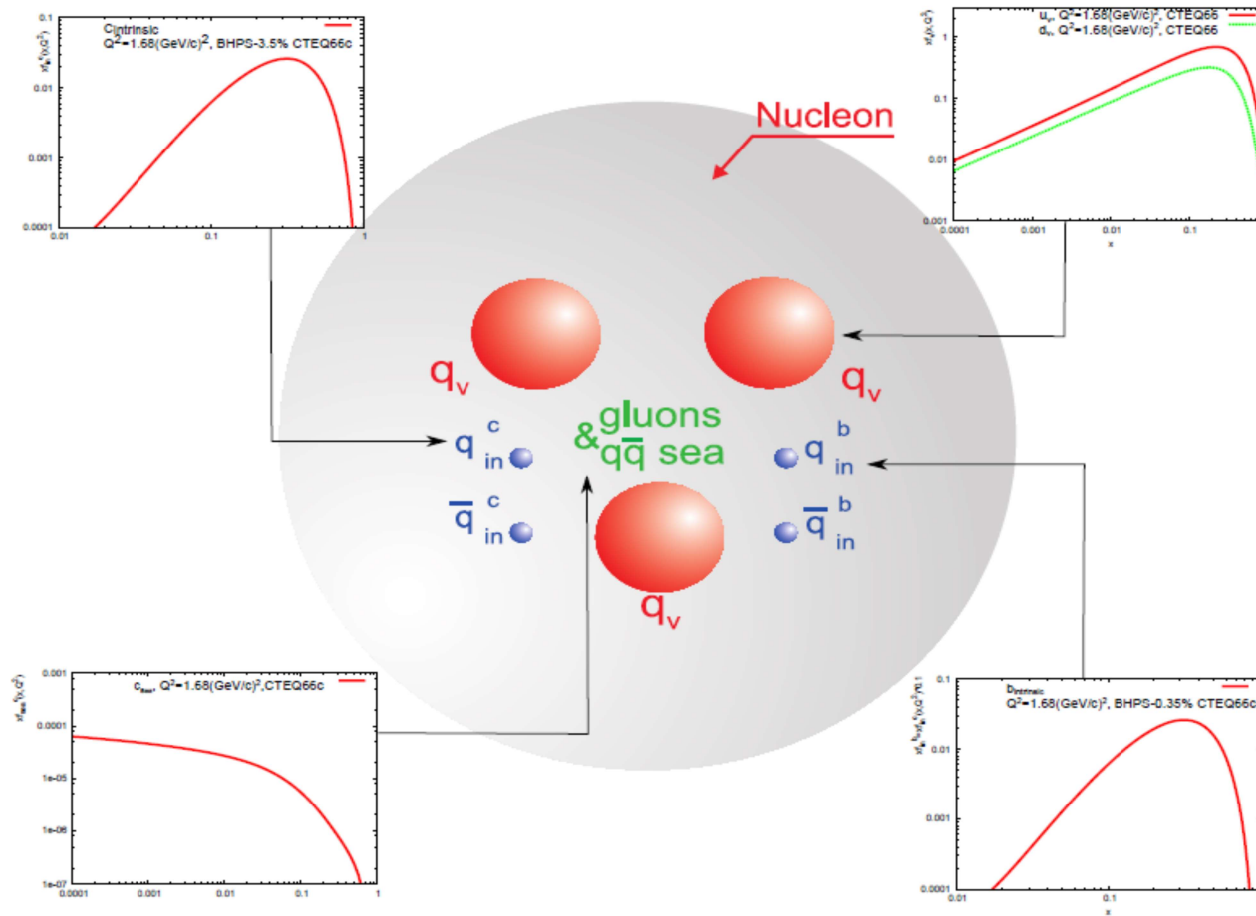


OUTLINE

- 1. Short overview of search for the **IQ** content in the proton.**
- 2. Lattice QCD results for the charm-anticharm asymmetry from $(c\bar{c})$ contribution to the electric form factor $G_{el}(x, Q^2)$ of proton.**
- 3. NNPDF Collaboration results for the IC indication at the c-jet – anti c-jet asymmetry in $pp \rightarrow Z + c(\bar{c})$ jets**
- 4. Asymmetric intrinsic charm-anticharm sea in a nucleon and D \bar{D} asymmetry in pp collisions.**
- 5. Summary.**

BHPS model: S.J. Brodsky, P. Hoyer, C. Peterson and N. Sakai, Phys.Lett.B9(1980) 451; S.J. Brodsky, S.J. Peterson and N. Sakai, Phys.Rev. D23 (1981) 2745.

Intrinsic $Q\bar{Q}$ in proton



INTRINSIC HEAVY QUARK STATES

Two types of parton contributions

The extrinsic quarks and gluons are generated on a short time scale in association with a large transverse-momentum reaction.

The intrinsic quarks and gluons exist over a time scale independent of any probe momentum, they are associated with the bound state hadron dynamics.

$$P(x_1, \dots, x_5) = N_5 \delta\left(1 - \sum_{i=1}^5 x_i\right) \left[M_p^2 - \sum_{i=1}^5 \frac{m_i^2}{x_i} \right]^{-2}$$

Non vanishing asymmetric charm-anticharm sea in a nucleon, as the IC confirmation

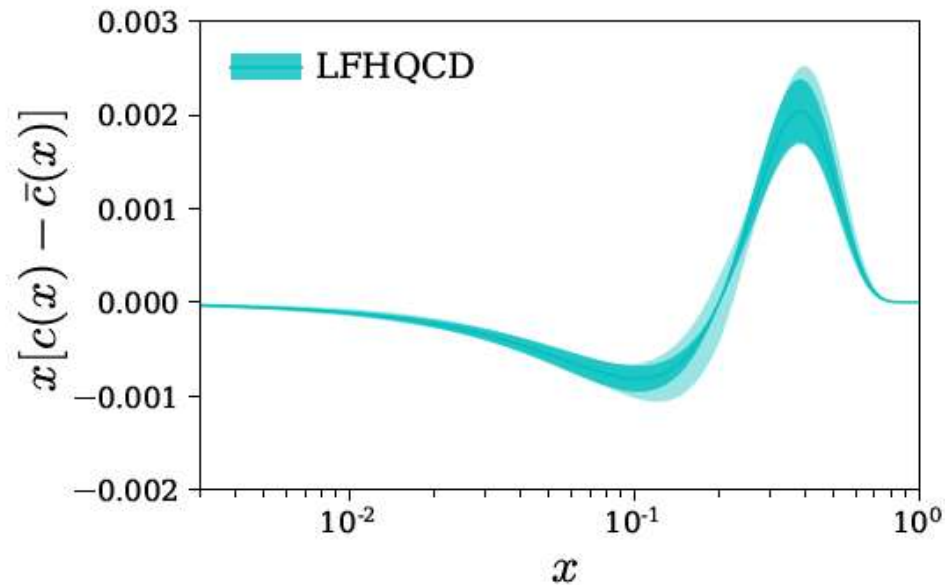


Figure 3: The distribution function $x[c(x) - \bar{c}(x)]$ obtained from the LFHQCD formalism using the lattice QCD input of charm electromagnetic form factors $G_{E,M}^c(Q^2)$. The outer cyan band indicates an estimate of systematic uncertainty in the $x[c(x) - \bar{c}(x)]$ distribution obtained from a variation of the hadron scale κ_c by 5%. It was taken from Ref. [1].

The nonzero

$G_E^c(Q^2)$ indicates the existence of a nonvanishing asymmetric charm-anticharm sea in the nucleon. Performing a non-perturbative analysis based on holographic QCD and the generalized Veneziano model, we study the constraints on the $[c(x) - \bar{c}(x)]$ distribution from the lattice QCD results presented here. Our results provide complementary information and motivation for more detailed studies of physical observables that are sensitive to intrinsic charm and for future global analyses of parton distributions including asymmetric charm-anticharm distribution.

Raza Sabbir Sufian, S. Brodsky, et al., Phys. Lett. B 808 (2020),135633

The intrinsic charm quark valence distribution of the proton

R.D.Ball, et al., NNPDF collaboration, arXiv:23110043 [hep-ph].

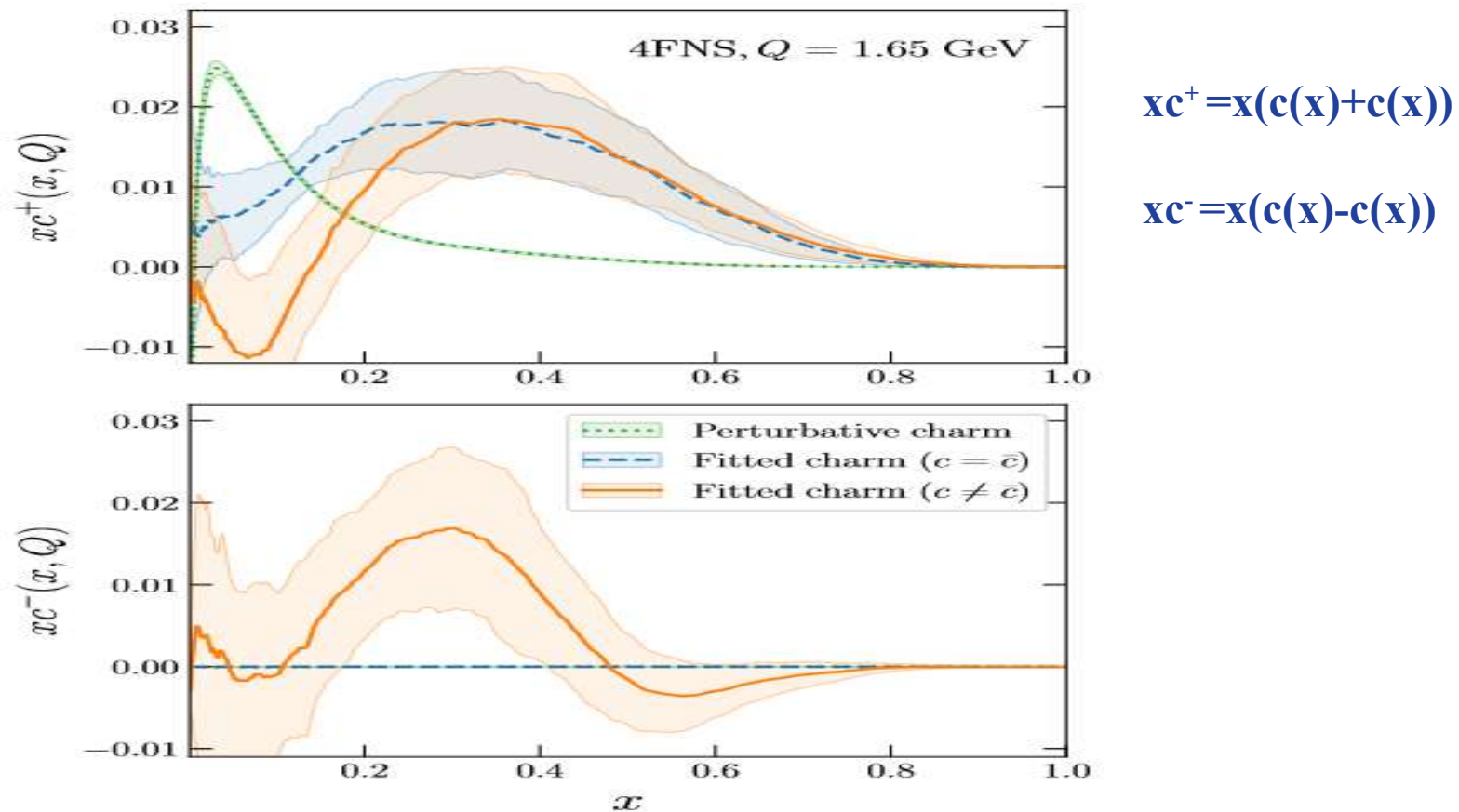


FIG. 1: The charm total $x c^+$ (top) and valence $x c^-$ (bottom) PDFs in the 4FNS at $Q = 1.65$ GeV. The perturbative and data-driven results are compared, in the latter case either assuming $c^- = 0$ (as in [9]) or c^- determined from data.

- [9] NNPDF Collaboration, R. D. Ball, A. Candido, J. Cruz-Martinez, S. Forte, T. Giani, F. Hekhorn, K. Kudashkin, G. Magni, and J. Rojo, *Evidence for intrinsic charm quarks in the proton*, *Nature* **608** (2022), no. 7923 483–487, [arXiv:2208.08372].

Quark diquark x -distributions within the QGSM

$$f_p^{uv(n)}(x) = C_n^{uv} x^{-\alpha_R(0)} (1-x)^{\alpha_R(0)-2\alpha_N(0)+n-1}, \quad (6)$$

$$G_d^{D^-}(x/x_1) = G_{\bar{u}}^{D^0}(x/x_1) = (1-x/x_1)^{\lambda-\alpha_\psi(0)} [1 + a_1(x/x_1)^2], \quad (7)$$

and the ud diquark has the following x -dependence:

$$f_p^{ud(n)}(x) = C_n^{ud} (1-x)^{-\alpha_R(0)} x^{\alpha_R(0)-2\alpha_N(0)+n-1}, \quad (8)$$

where $\alpha_R(0) = 0.5$, $\alpha_N(0) = -0.5$, $\alpha_\psi(0) = -2.2$, $\lambda = 2 < p_{\perp}^2 > \alpha'_R = 0.5$, and the coefficient C_n^{uv} is determined by normalization $\int_0^1 f_p^{uv(n)}(x) dx = 1$. One can see from Eqs. (6,8) that the diquark distribution increases as $(1-x)^{-\alpha_R(0)}$ and the valence quark distribution decreases as $(1-x)^{\alpha_R(0)-2\alpha_N(0)+n-1}$ when x grows.

The distribution of the sea charmed quark in proton has the following form:

$$f_{c\bar{c}}^{(n)} = C_{c\bar{c}} \delta_{c\bar{c}} x^{a_c} (1-x)^{b_c^n},$$

where $a_c = -\alpha_\psi(0)$ and $b_c^n = 2\alpha_R(0) - 2\alpha_N(0) - \alpha_\psi(0) + n - 1$

Intrinsic charm (IC)

$$f_{c\bar{c}}^{(n)}(x) \rightarrow (1-w) f_{c\bar{c}}^{(n)}(x) + w f_{c\bar{c}}^{in}(x), \quad (13)$$

where w is the probability of the IC contribution in proton and $f_{c\bar{c}}^{in}$ is the intrinsic charm contribution to the conventional charm distribution at $n \geq 2$

Symmetric IC

$$f_{c\bar{c}}^{in}(x) = 600x^2 \{ (1-x)(x^2 + 10x + 1) + 6x(x+1)\ln(x) \} ,$$

with the normalization condition

$$\int_0^1 f_{c\bar{c}}^{in}(x) dx = 1.$$

Asymmetric IC

$$f_c^{in}(x) = Ax^{1.897}(1-x)^{6.095} \quad (16)$$

and

$$f_{\bar{c}}^{in}(x) = \bar{A}x^{2.5}(1-x)^{4.929} , \quad (17)$$

where A/\bar{A} is determined by the quark number sum rule :

$$\int_0^1 \{ f_c^{in}(x) - f_{\bar{c}}^{in}(x) \} dx = 0 . \quad (18)$$

We used (16) for $f_c^{in}(x)$ and $f_{\bar{c}}^{in}(x)$ was calculated as

$$f_{\bar{c}}^{in}(x) = f_c^{in}(x) - \Delta c(x) ,$$

where the difference $\Delta c(x) = [c(x) - \bar{c}(x)]$ was taken from

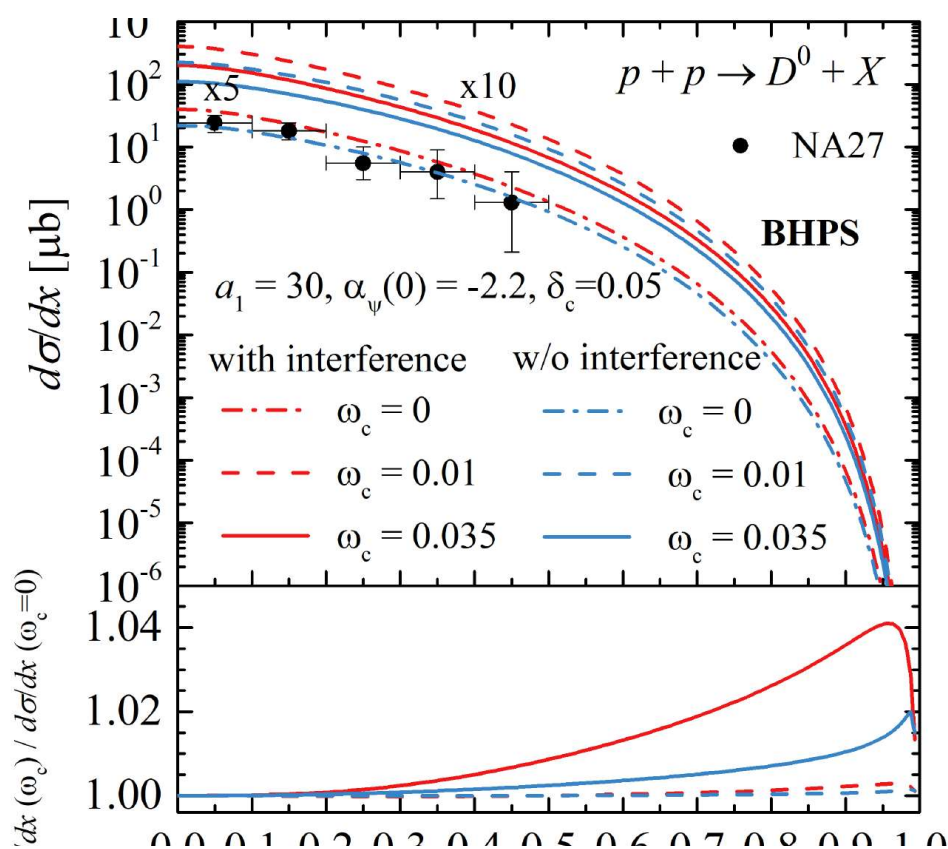


Figure 1: The x -distribution of the inclusive spectrum of D^0 -mesons produced in pp collisions at the initial energy $E_{lab} = 400$ GeV and $0 \leq x \leq 1$. Top: the inclusive spectrum at different values of ω with and without (w/o) the interference of the quark (diquark) and the sea quark (extrinsic and intrinsic) amplitudes. The interference between the extrinsic and intrinsic quark contributions are also taken into account; see Appendix. The NA27 data were taken from [27]. Bottom: the ratio of the x -spectrum for the nonzero IC probability ω_c to the spectrum at $\omega_c = 0$, with interference and without it. With interference: solid red line at $\omega_c = 0.035$, dashed red line at $\omega_c = 0.01$. Without interference (w/o): solid blue line at $\omega_c = 0.035$, dashed blue line at $\omega_c = 0.01$. The calculations were done using the IC distributions in forms of Eqs.(16,17), labeled as **BHPS**.

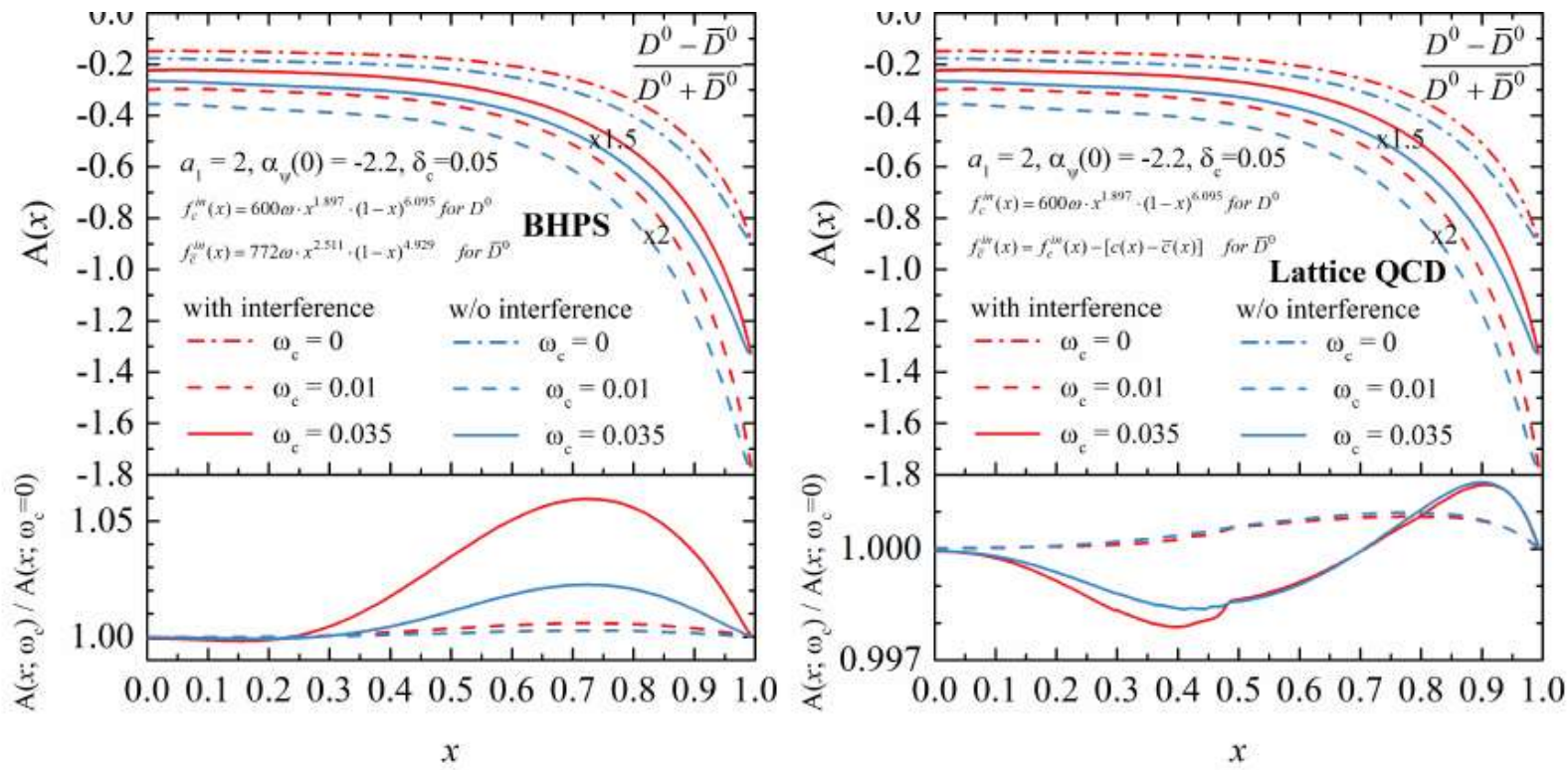


Figure 3: Left: the *Set 1* of x -distribution of asymmetry $A_{D^0\bar{D}^0}(x)$ between D^0 and \bar{D}^0 -mesons produced in pp collision at the initial energy $E_{lab} = 400$ GeV and $a_1 = 2$, and the ratio of the asymmetry with the non zero IC probability ω_c to the one with $\omega_c = 0$. The calculations were done using the IC distributions in forms of Eqs.(16,17). Right: the *Set 2* of asymmetry $A_{D^0\bar{D}^0}(x)$ using Eq.(16) for $f_c^{in}(x)$ and Eq.(17) for $f_{\bar{c}}^{in}(x)$. With interference: solid red line at $\omega_c = 0.035$, dashed red line at $\omega_c = 0.01$. Without interference (w/o): solid blue line at $\omega_c = 0.035$, dashed blue line at $\omega_c = 0.01$.

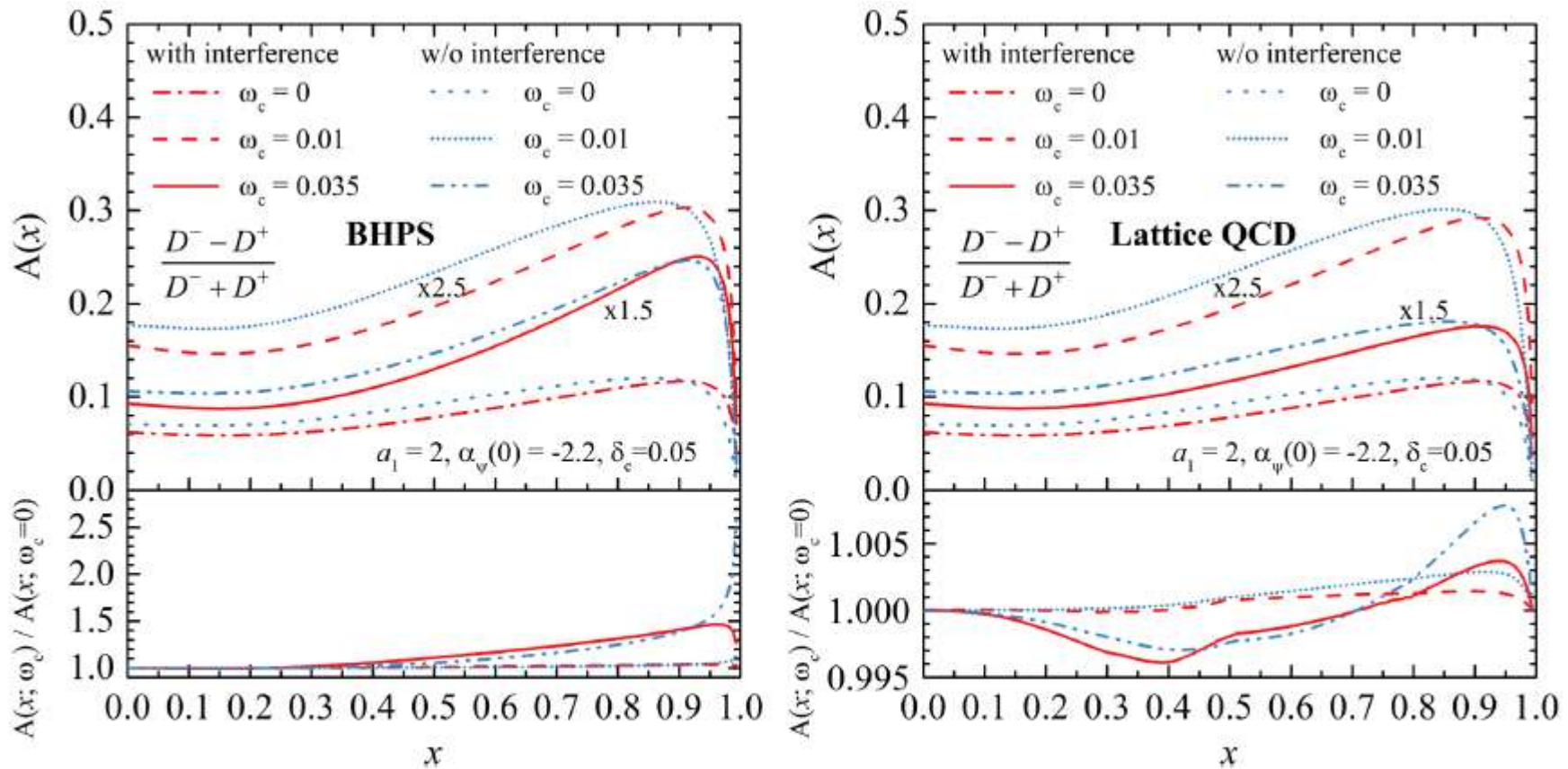


FIG. 4. The plots for asymmetry $A_{D^-D^+}(x)$ with the same notations as in Fig. 3.

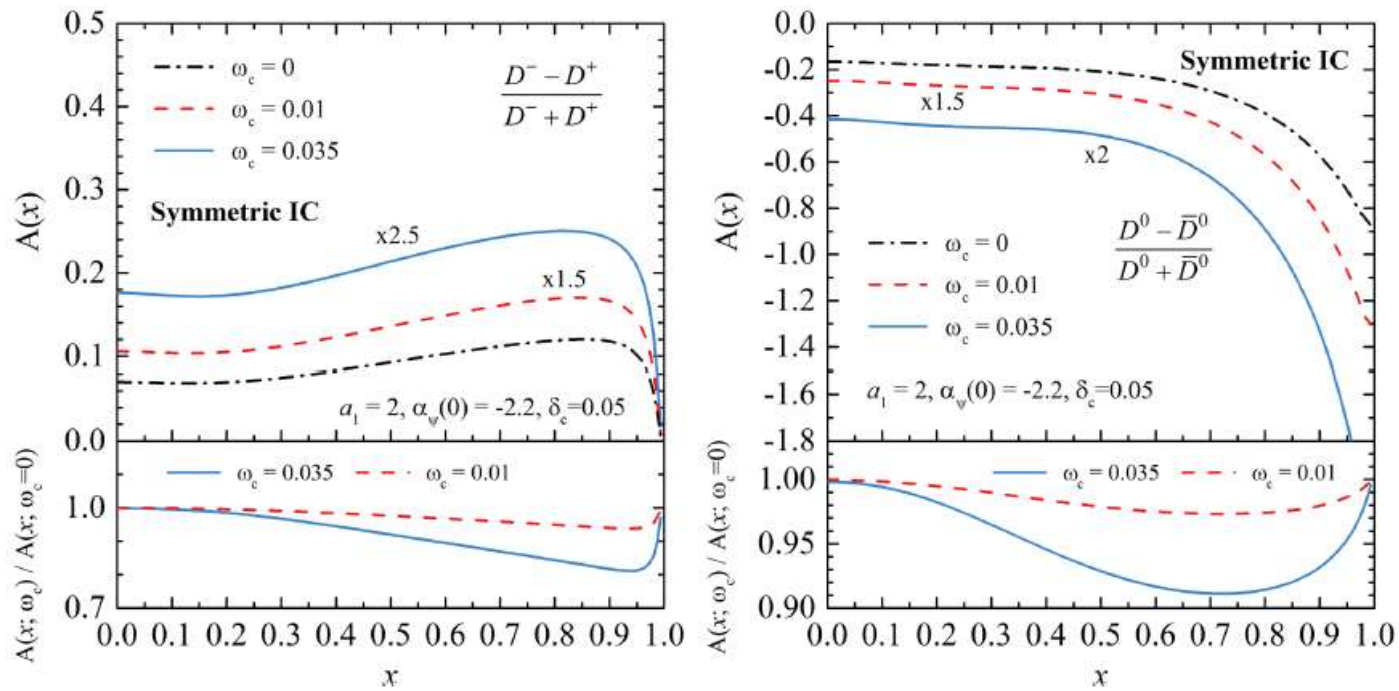


FIG. 5. The plots of the asymmetries $A_{D^-D^+}(x)$ (left) and $A_{D^0\bar{D}^0}(x)$ (right) using the symmetric *IC* distribution, according to Eq. (13) with the same notations as in Fig. 3.

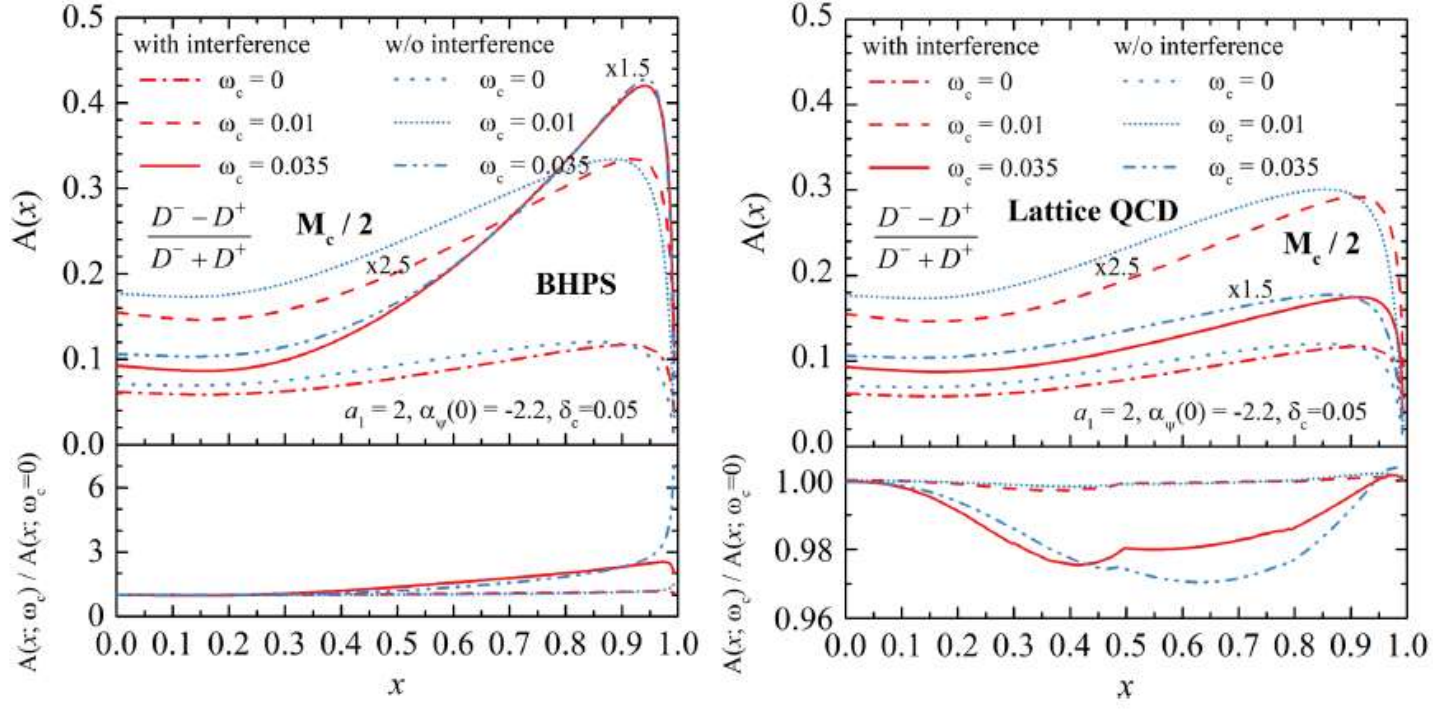


FIG. 6. The plots of the asymmetry $A_{D^-D^+}(x)$ for the mass of intrinsic quark $M_Q = M_c/2$ with the same notations as in Fig. 3.

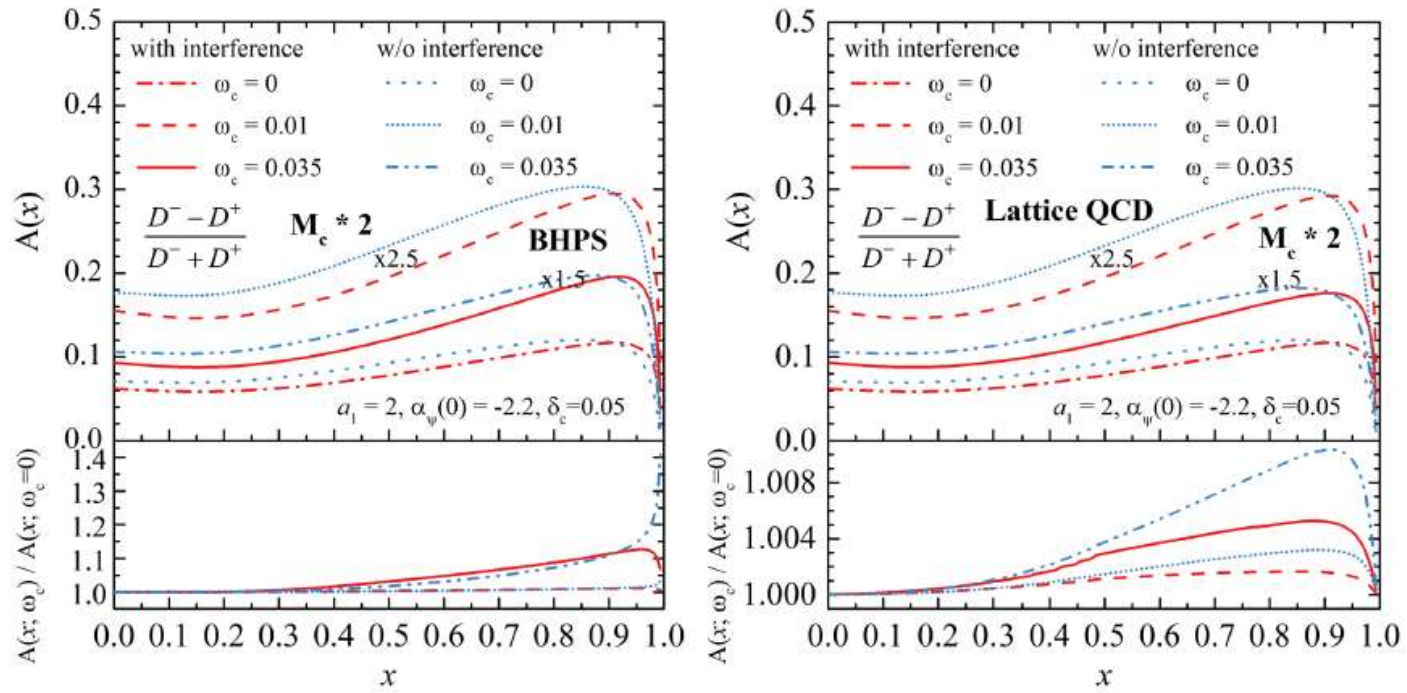


FIG. 7. The plots of the asymmetry $A_{D^-D^+}(x)$ for the mass of intrinsic quark $M_Q = M_c * 2$ with the same notations as in Fig. 3.

SUMMARY

1. The lattice QCD calculation shows that the charm quark contribution to the electric form factor of proton doesn't vanish. It leads to the non vanishing asymmetry $c(x) - \bar{c}(x)$, which can indicate the **IC existence in nucleon**.
2. Using these results we calculated the asymmetry for D^- and D^+ D^0 and \bar{D}^0 produced in pp collisions.
3. Maximum value of D^-D^+ asymmetry, including the **IC** contribution, can be about 40 % at $\omega_{IC} = 3.5\%$ and $x = 0.85-0.90$.
However, the maximum of the $D^0 \bar{D}^0$ asymmetry is about (5-6)% at $x = 0.8$.
4. The contribution of the **IC** content to inclusive spectrum is too low because there is cancellation of these contributions in difference $\sigma(D^0) - \sigma(\bar{D}^0)$, which is due to big contribution of the diquark distribution at large x (about $1/\{(1-x)^{1/2}\}$).
5. The D^-D^+ asymmetry using the symmetric **IC changes the sign for asymmetric IC**.
6. The measurement of $(\sigma(D^-) - \sigma(D^+)) / (\sigma(D^+) + \sigma(D^-))$ as a function of x_F is very promising for the search for the charm-anticharm quark asymmetry, which could be very good confirmation of the existence of the **IC** component in nucleon.

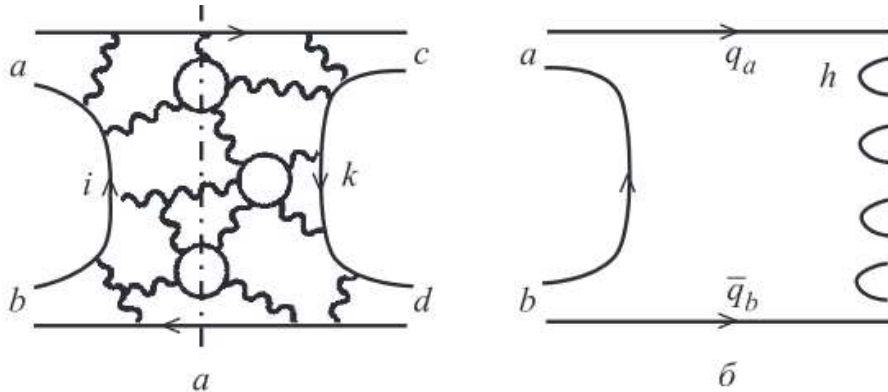
**THANK YOU VERY MUCH FOR
YOUR ATTENTION !**

BACK UP

Topological $1/N$ expansion, when $\alpha_s N_c = \text{constant}$

't Hooft G. — Nucl. Phys., 1974, v.B72, p.461.

Planar graphs in the s-channel

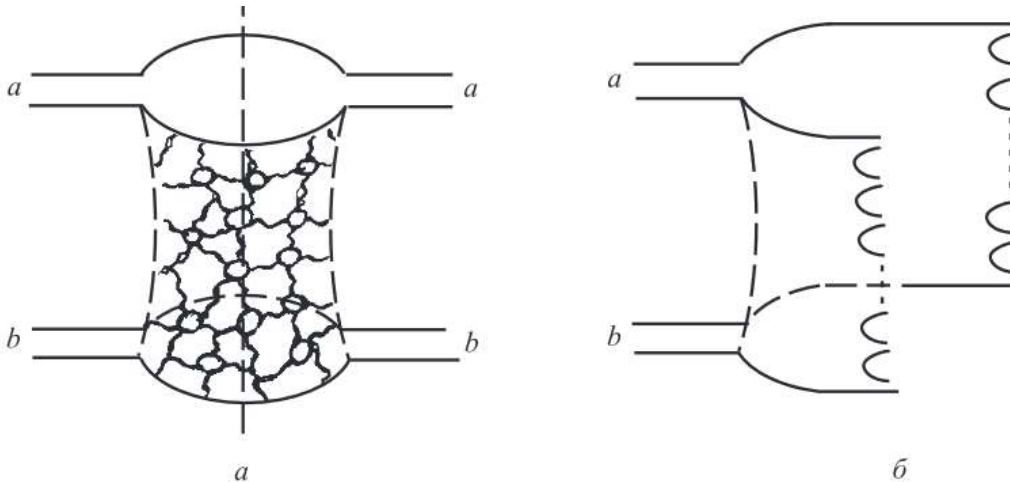


$$T_{ab \rightarrow cd}^{(h=0, b=1)} \propto \frac{1}{N_f} \propto \frac{1}{N_c}.$$

It is equivalent to the one-Reggion exchange in the t-channel.

This contribution results in σ is proportional to $1/s^{1/2}$

Cylinder graphs in the s-channel



$$T_{ab \rightarrow ab}^{(h=0, b=2)} \propto \frac{1}{N_f^2} \propto \frac{1}{N_c^2}.$$

It is equivalent to the one-Pomeron exchange in the t-channel.

This contribution results in σ is proportional to s^Δ , where $\Delta = \alpha_p - 1 = 0.1-0.15$

$$\rho_h(x) = \int E \frac{d^3\sigma}{d^3p} d^2p_\perp = \sum_{n=0}^{\infty} \sigma_n(s) \varphi_n^h(s, x),$$

where $\sigma_n(s)$ is the cross section of the $2n$ -strings (chains) production

$$\varphi_n^D(s, x) = a^D \left\{ F_{qv}^{D(n)}(x_+) F_{qq}^{D(n)}(x_-) + F_{qq}^{D(n)}(x_+) F_{qv}^{D(n)}(x_-) \right. \\ \left. + 2(n-1) F_{q_{\text{sea}}}^{D(n)}(x_+) F_{\bar{q}_{\text{sea}}}^{D(n)}(x_-) \right\},$$

where $x_\pm(s) = \frac{1}{2} \left[\sqrt{x^2 + 4m_\perp^2/s} \pm x \right]$.

$$F_{qv}^{D(n)}(x_\pm) = \frac{2}{3} \int_{x_\pm}^1 f_p^{uv(n)}(x_1) G_u^D(x_\pm/x_1) dx_1 + \\ + \frac{1}{3} \int_{x_\pm}^1 f_p^{dv(n)}(x_1) G_d^D(x_\pm/x_1) dx_1,$$

PP-→K-X

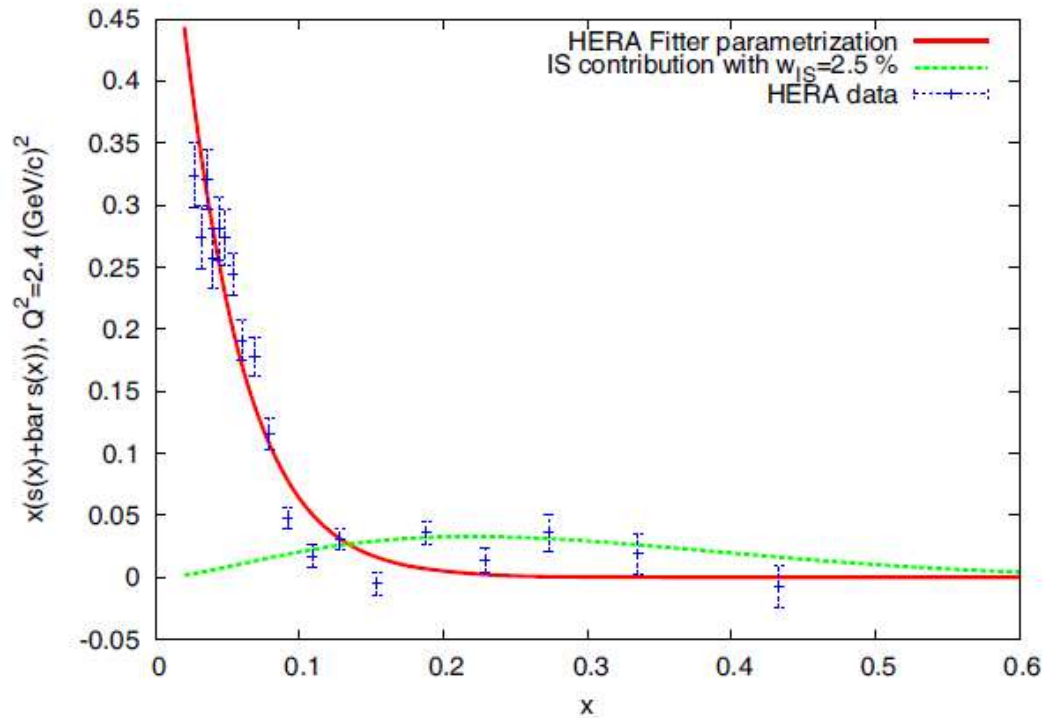


Figure 2: The distributions of strange quarks $xS(x) = x(s(x) + \bar{s}(x))$ in the proton; the solid line is the HERA Fitter parametrization of $xS(x)$ at $Q^2 = 2.4 \text{ GeV}/c$, the dashed curve is the contribution of the *intrinsic* strangeness (IS) in the proton with the probability 2.5 %. The HERA data were taken from [16].

[16] A.Airapetian, HERMES Collaboration, Phys.Lett.B666:446-450,2008; arXiv:0803.2993 [hep-ex].

G.L., I.V. Bednyakov, M.A. Demichev, Yu.Yu. Stepanenko,
Nucl.Phys. B (Proc.Suppl.) 245, 213 (2013)

5. Discussion on the asymmetry of neutrino-antineutrino, produced from D-meson decays.

Application for FASER experiment at CERN

6. Intrinsic strangeness in the proton and its search for different experiments

Application for SPD experiment at JINR

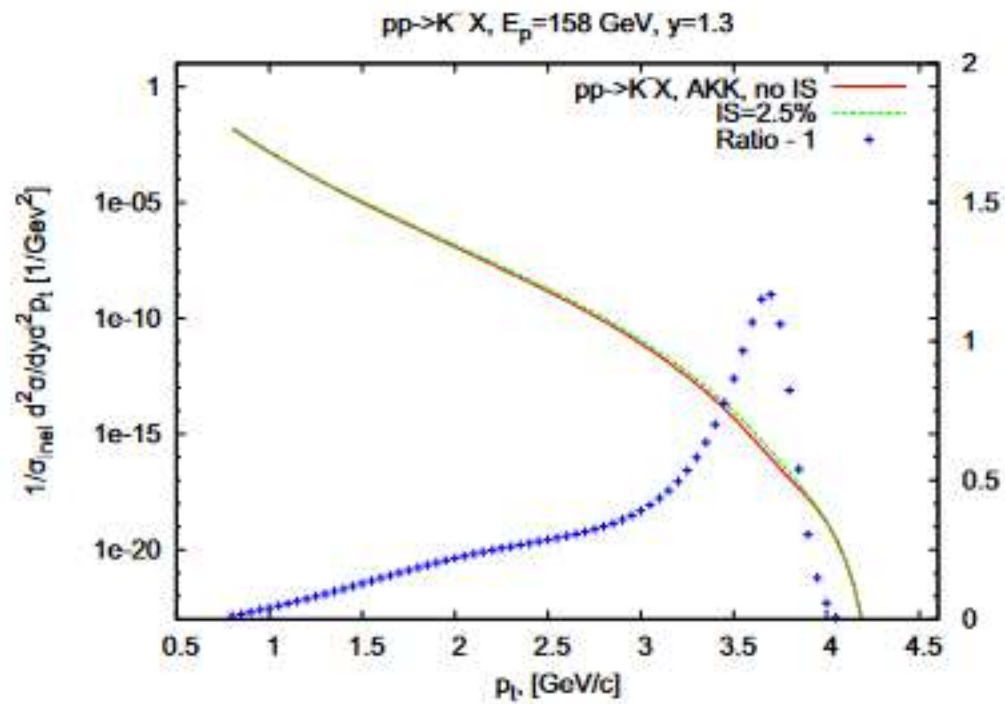


Figure 4: The K^- -meson distributions (with and without intrinsic strangeness contribution) over the transverse momentum p_t for $pp \rightarrow K^- + X$ at the initial energy $E = 158 \text{ GeV}$, the rapidity $y = 1.3$ and $p_t \geq 0.8 \text{ GeV}/c$.

**G.L., I.V. Bednyakov, M.A. Demichev, Yu.Yu. Stepanenko,
Nucl.Phys. B (Proc.Suppl.) 245, 213 (2013)**

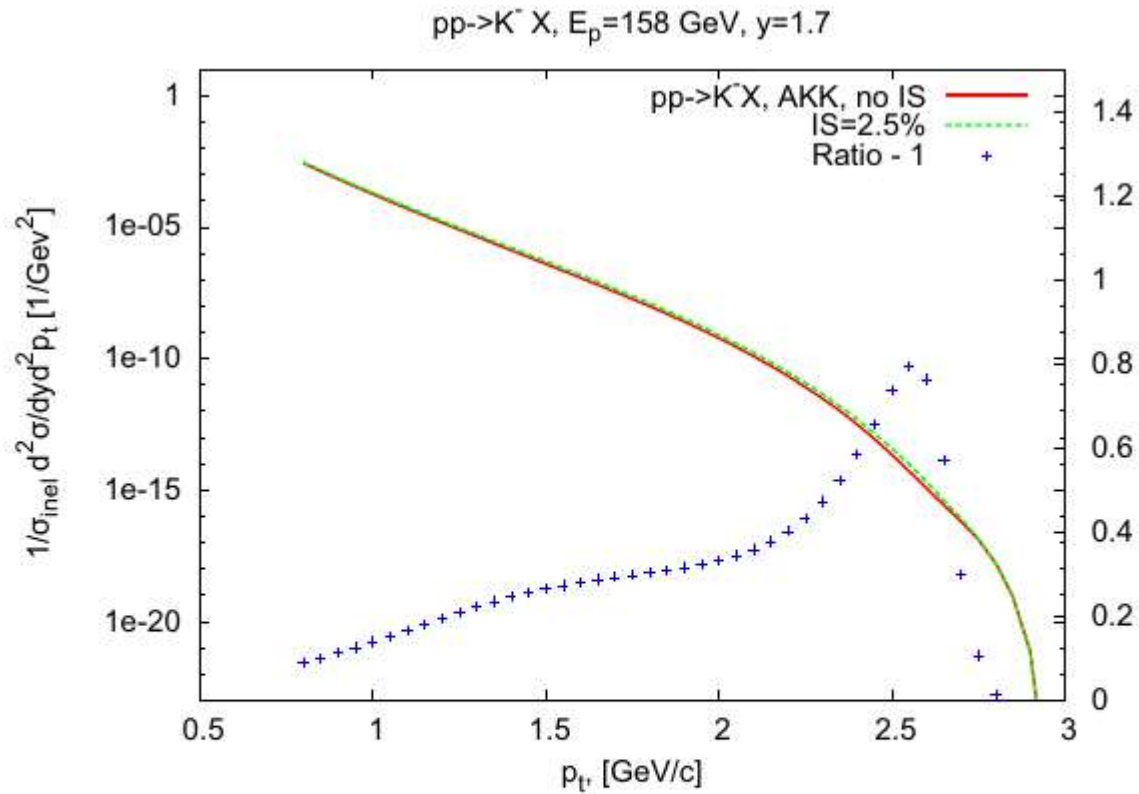


Figure 5: The K^- -meson distributions (with and without intrinsic strangeness contribution) over the transverse momentum p_t for $pp \rightarrow K^- + X$ at the initial energy $E = 158$ GeV, the rapidity $y = 1.7$ and $p_t \geq 0.8$ GeV/c.

G.L., I.V. Bednyakov, M.A. Demichev, Yu.Yu. Stepanenko,
Nucl.Phys. B (Proc.Suppl.) 245, 213 (2013)

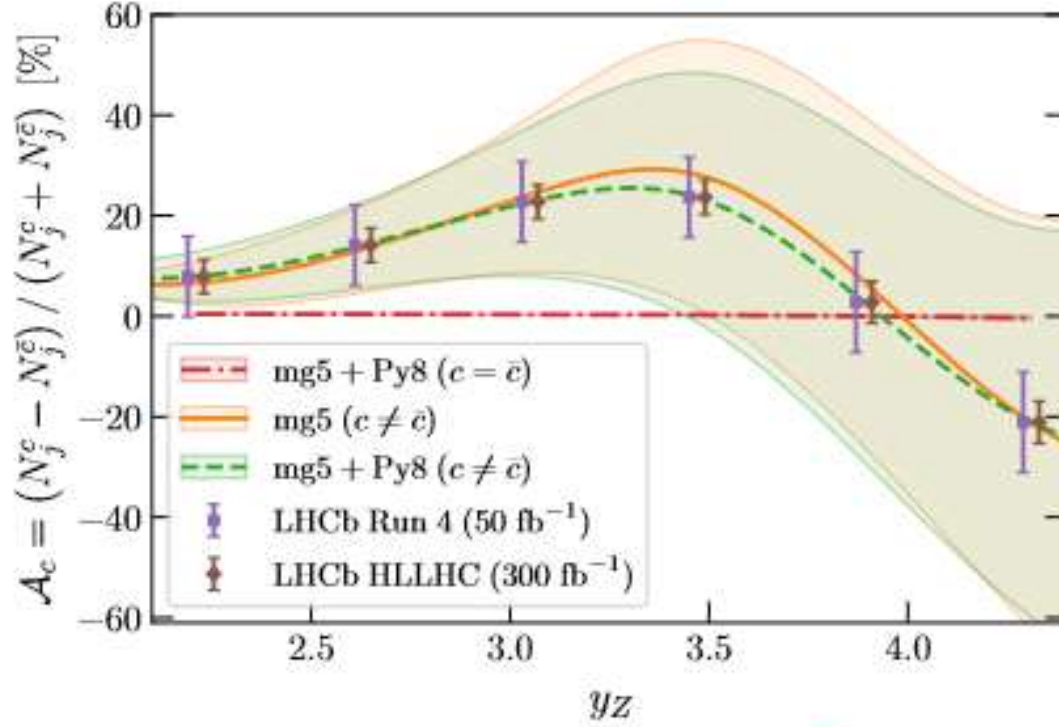


FIG. 3: The charm asymmetry $\mathcal{A}_c(y_Z)$, Eq. (1), in $Z+c$ -jet production at LHCb ($\sqrt{s} = 13 \text{ TeV}$) evaluated at LO matched to parton showers with the nonvanishing valence PDF determined here. The pure LO result and the result with vanishing charm valence are also shown for comparison. The bands correspond to one-sigma PDF uncertainties. Projected statistical uncertainties for LHCb measurements at Run 4 ($\mathcal{L} = 50 \text{ fb}^{-1}$) and the HL-LHC ($\mathcal{L} = 300 \text{ fb}^{-1}$) are also shown.

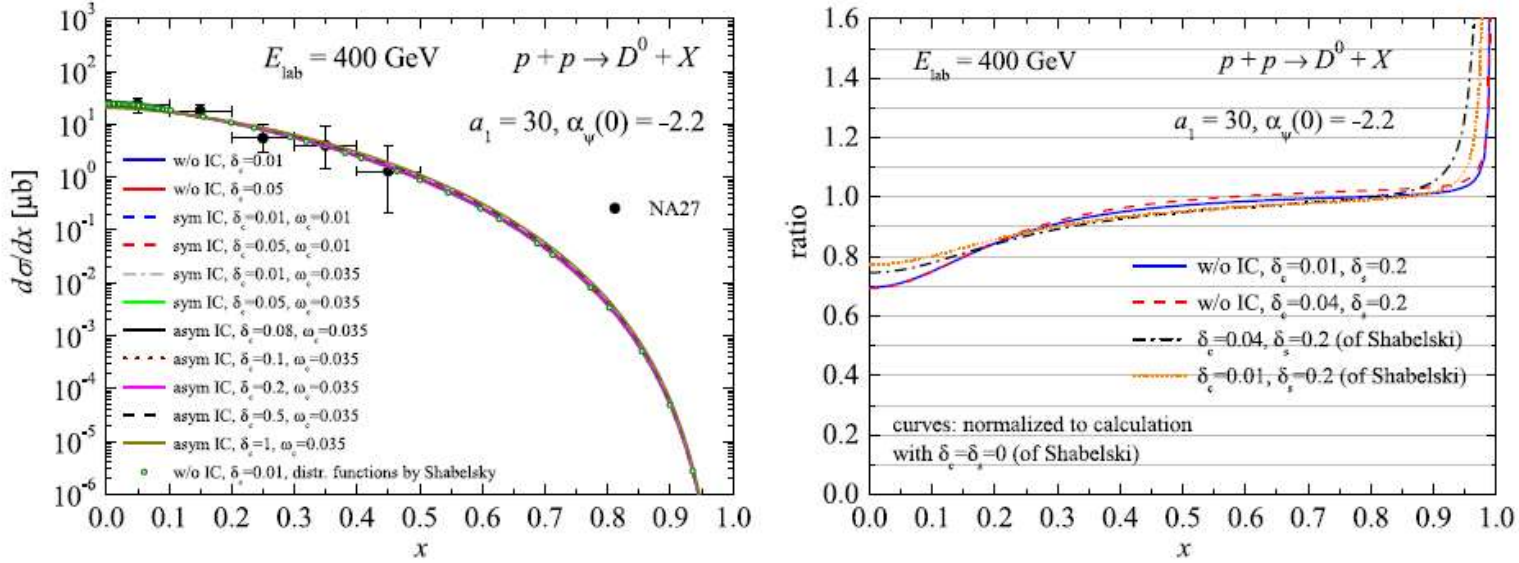


FIG. 2. Left: our calculation of the inclusive x -spectrum of D^0 -mesons produced in pp collisions at the initial energy $E_{\text{lab}} = 400 \text{ GeV}$ with different values of the weight δ_c and the IC probability w_c . The open circles correspond to the calculation of Ref. [37]. Right: the blue solid line is the ratio R_1 , the red dashed line is R_2 , the black dot-dashed line is R_3 , and the orange dotted line is R_4 .

Electro-magnetic form factors within the lattice QCD

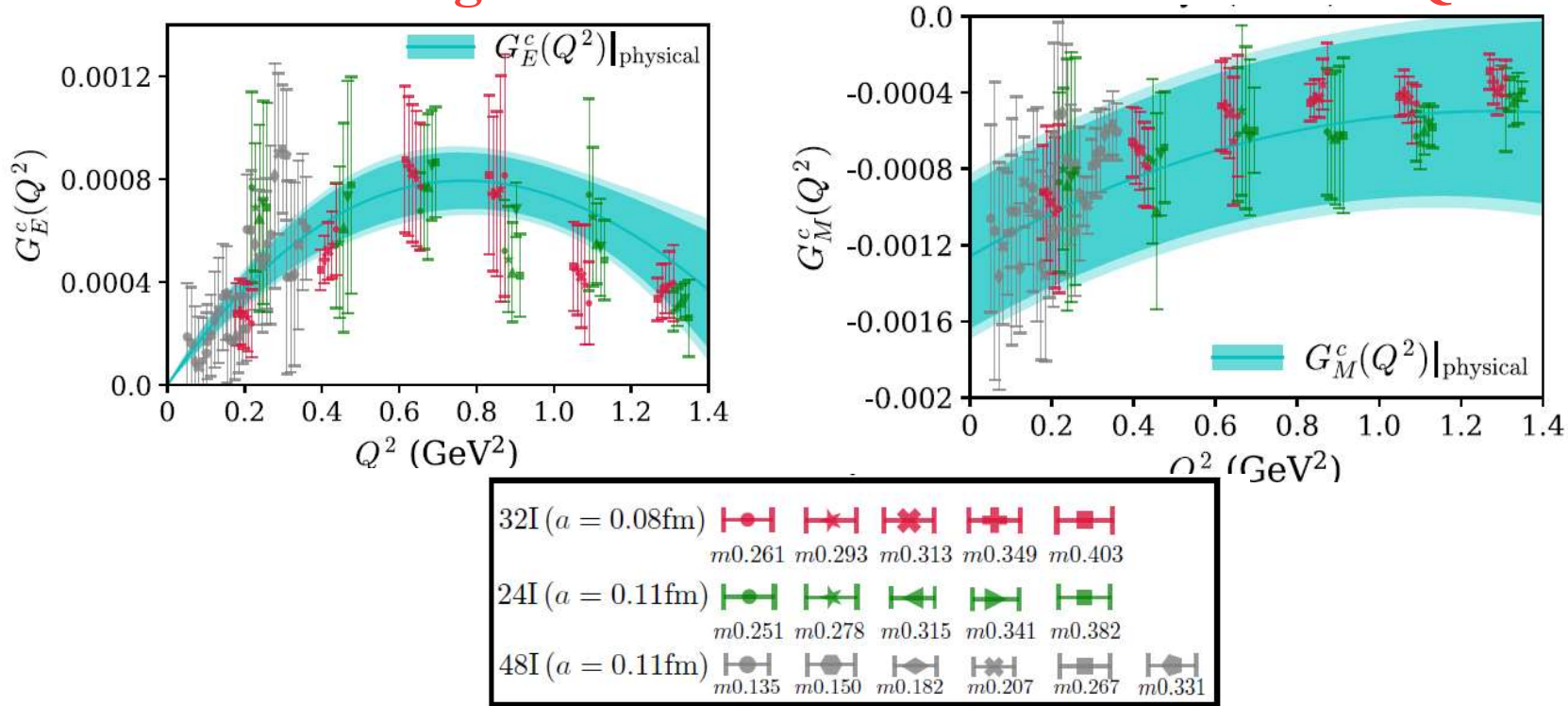


Figure 2: $G_{E,M}^c(Q^2)$ matrix elements obtained from the 48I, 32I, and 24I ensembles. Corresponding legends for different pion masses are included in the lower panel of the figure. The numbers in the legends, such as $m139$, $m251$ represent the data points corresponding to pion mass 139 MeV and 251 MeV, respectively at different Q^2 -values. The cyan band indicates $G_{E,M}^c(Q^2)|_{\text{physical}}$. The outer (lighter tinted) cyan margins represent an estimate of systematic uncertainty. Matrix elements at the same Q^2 -value but at different pion masses are shown with small offsets for better visibility.

Raza Sabbir Sufian, S. Brodsky, et al., Phys. Lett. B 808 (2020),135633

Intrinsic strangeness (IS)

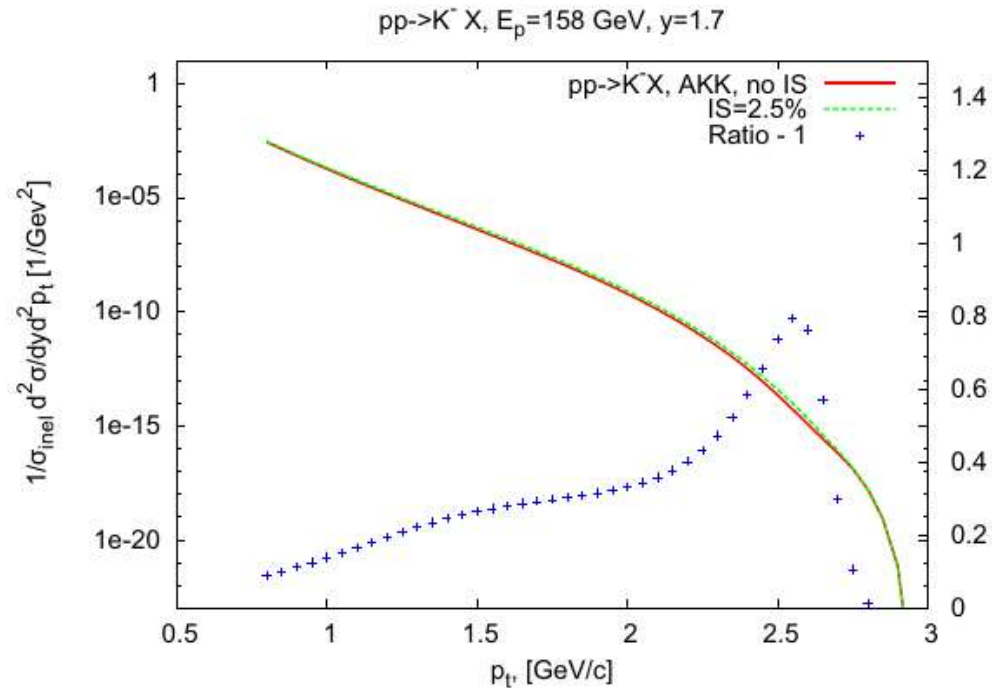
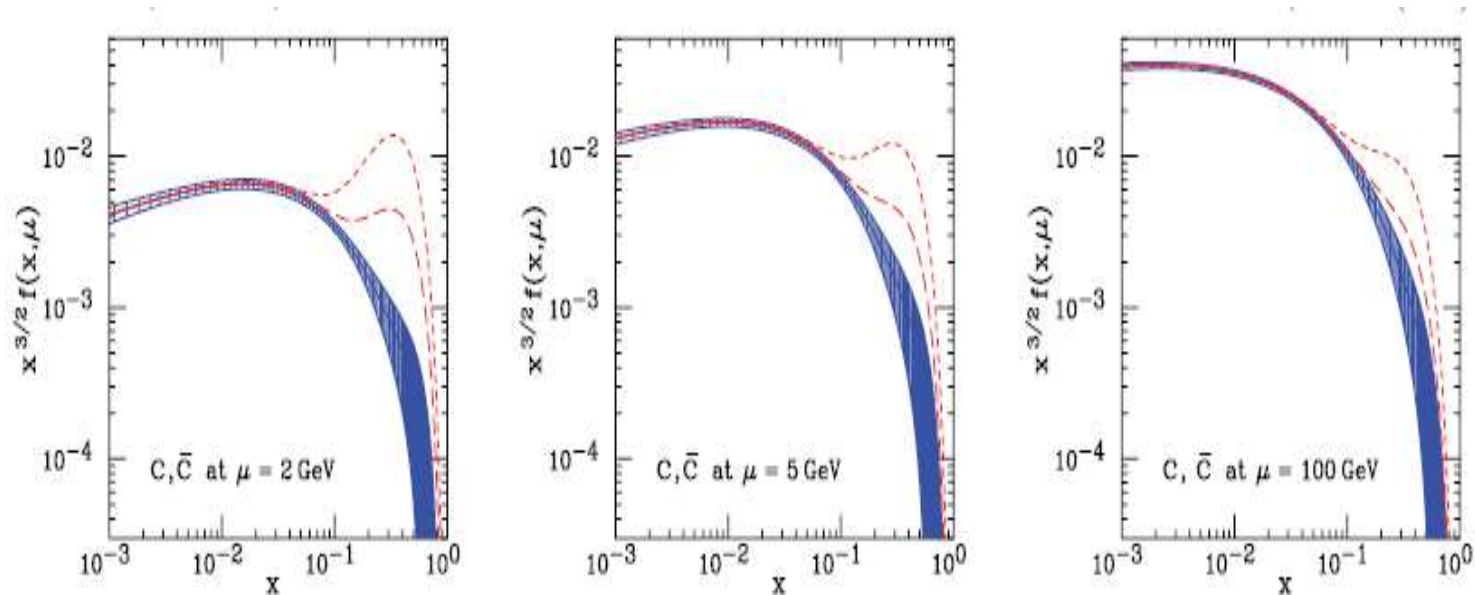


Figure 5: The K^- -meson distributions (with and without intrinsic strangeness contribution) over the transverse momentum p_t for $pp \rightarrow K^- + X$ at the initial energy $E = 158$ GeV, the rapidity $y = 1.7$ and $p_t \geq 0.8$ GeV/c.

G.L., I.V. Bednyakov, M.a. ITVBXTV., Yu.Yu. Stepanenko,
Nucl.Phys. B(Proc.Suppl.) v .245, p.215 (2013).

CHARM QUARK DISTRIBUTIONS IN PROTON



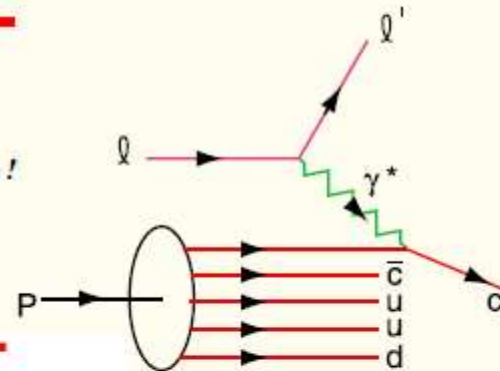
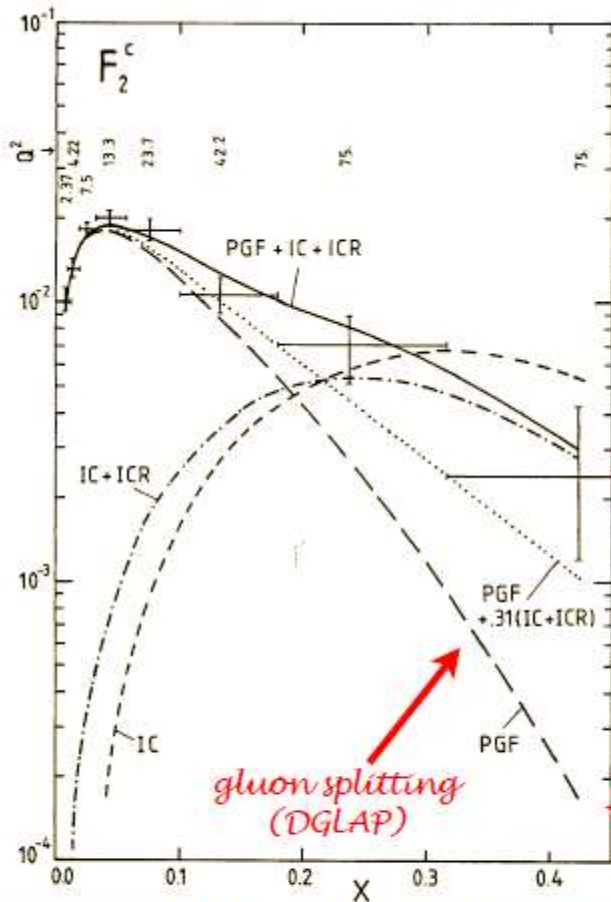
Charm quark distributions within the BHPS model. The three panels correspond to the renormalization scales $\mu = 2, 5, 100$ GeV respectively. The long-dashed and the short-dashed curves correspond to $x_{cc} = (0.57-2.)\%$ respectively using the PDF CTEQ66c. The solid curve and shaded region show the central value and uncertainty from CTEQ6.5, which contains no *IC*.

There is an enhancement at $x > 0.1$ due to the IC contribution

Measurement of Charm Structure Function

J. J. Aubert et al. [European Muon Collaboration], "Production Of Charmed Particles In 250-GeV Mu⁺ - Iron Interactions," Nucl. Phys. B 213, 31 (1983).

First Evidence for Intrinsic Charm



DGLAP / Photon-Gluon Fusion: factor of 30 too small

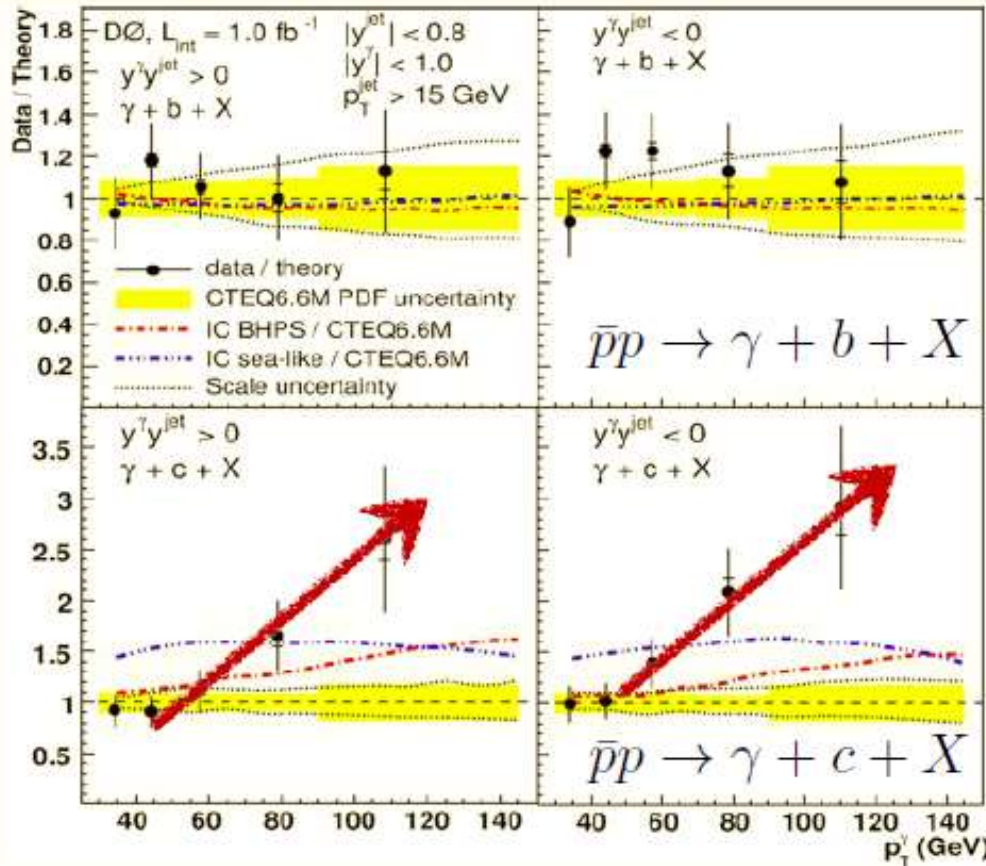
Two Components (separate evolution):

$$c(x, Q^2) = c(x, Q^2)_{\text{extrinsic}} + c(x, Q^2)_{\text{intrinsic}}$$

D0

Measurement of $\gamma + b + X$ and $\gamma + c + X$ Production Cross Sections
in $p\bar{p}$ Collisions at $\sqrt{s} = 1.96$ TeV

$$p\bar{p} \rightarrow \gamma + Q + X$$



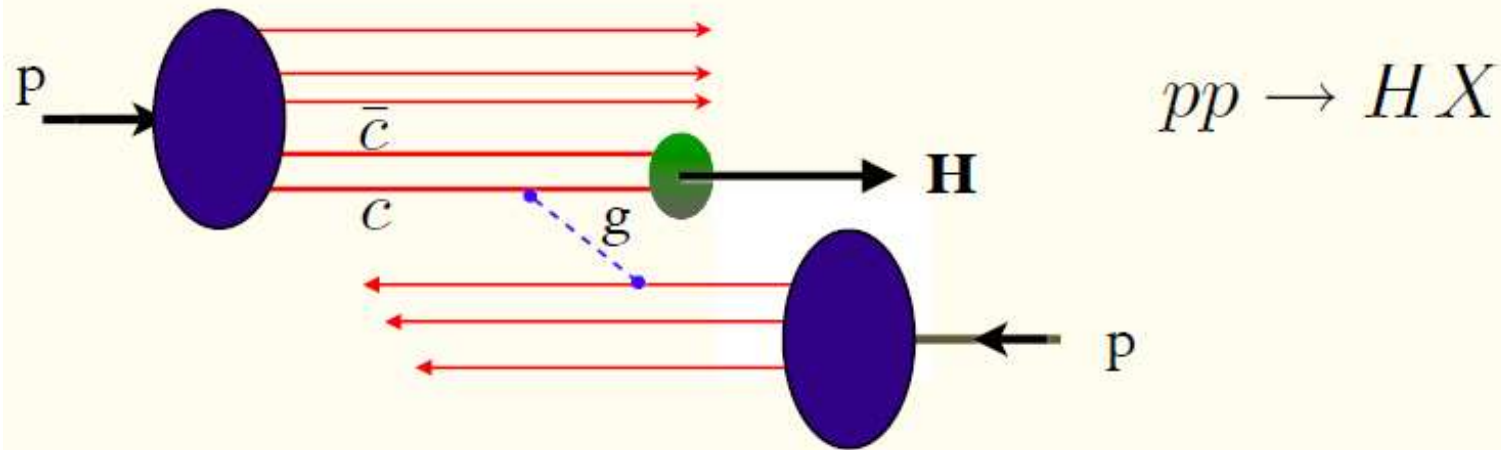
$$\frac{\Delta\sigma(\bar{p}p \rightarrow \gamma cX)}{\Delta\sigma(\bar{p}p \rightarrow \gamma bX)}$$

**Ratio is insensitive
to gluon PDF,
scales**

Consistent with $\frac{m_c^2}{m_b^2}$
relative suppression
of intrinsic bottom

$$c(x, Q^2) = c(x, Q^2)_{\text{extrinsic}} + c(x, Q^2)_{\text{intrinsic}}$$

Intrinsic Charm Mechanism for Inclusive High- x_F Higgs Production



Also: intrinsic bottom, top

**Goldhaber, Kopeliovich,
Schmidt, sjb**

Higgs can have 80% of Proton Momentum!

New search strategy for Higgs

Higgs production is equal from the IC and IB

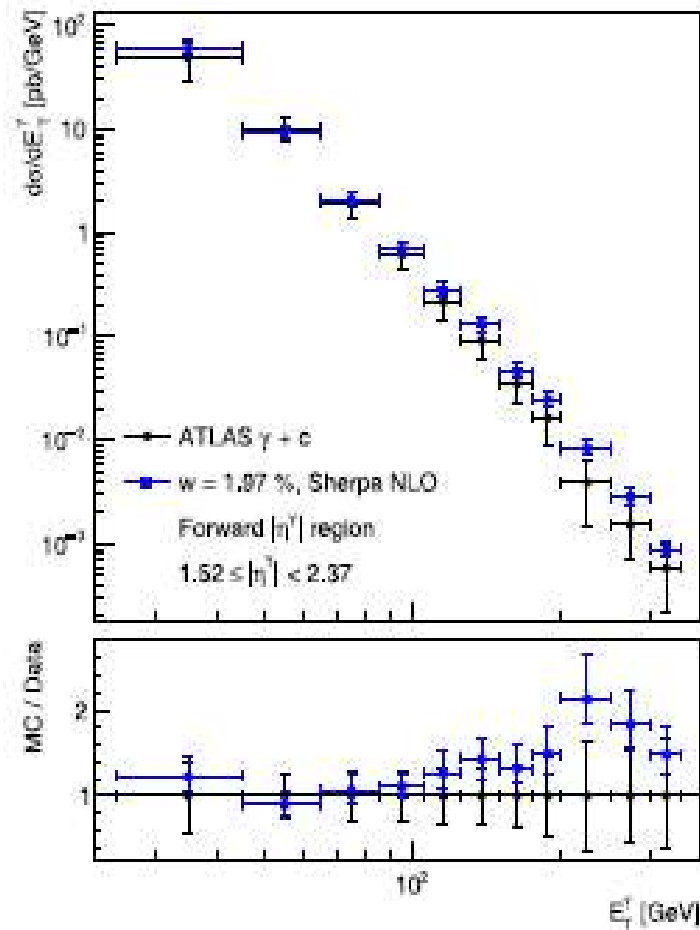
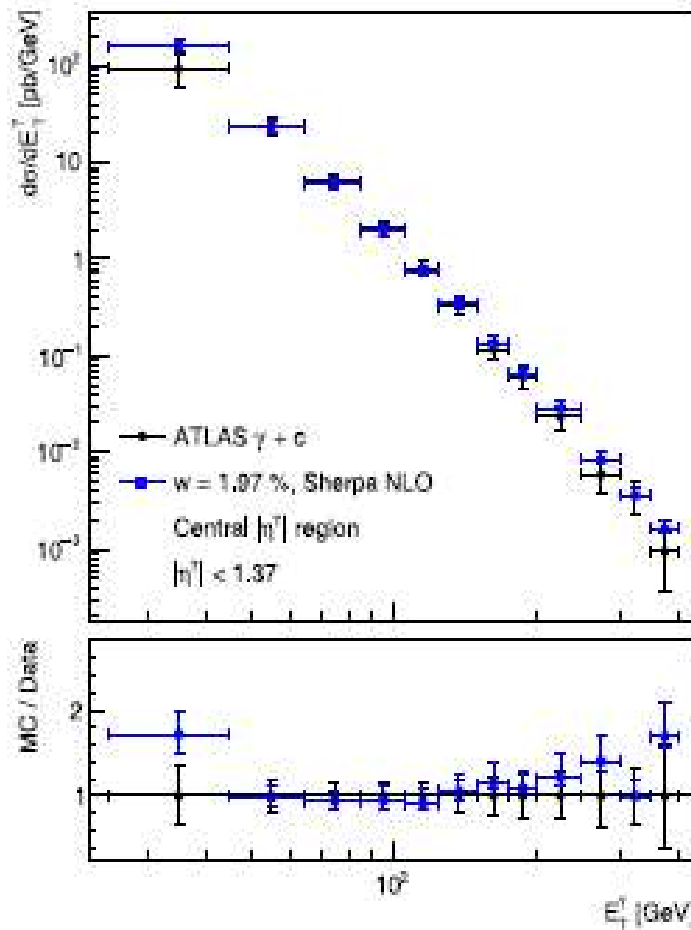
$p+p \rightarrow \gamma+c\text{-jet}+X$ at $s^{1/2} = 8$ TeV, ATLAS data

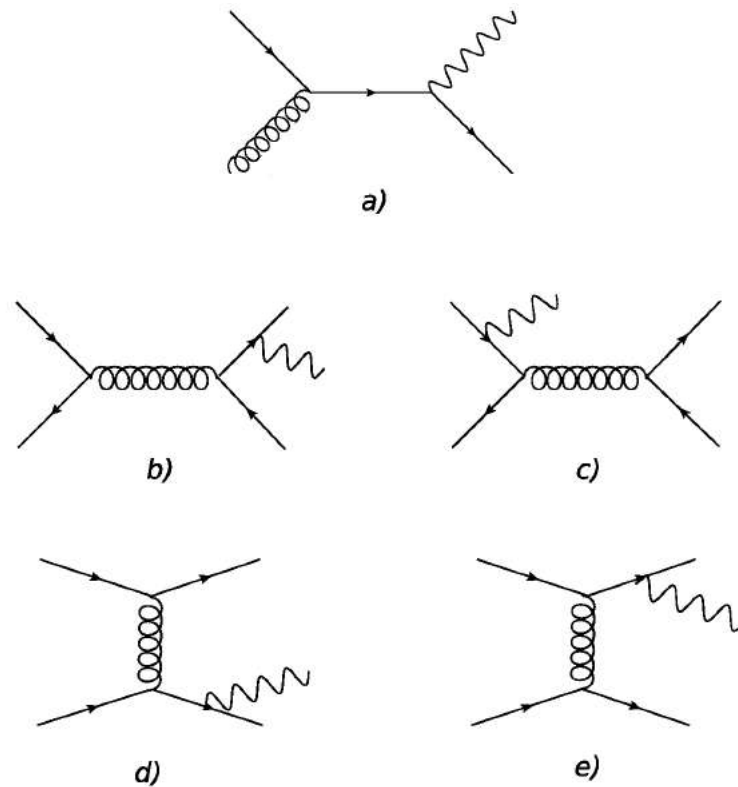
the upper limit of the **IC** probability is about 1.97%

V.A. Bednyakov, S. J. Brodskiy, A.V. Lipatov, G.L., M.A. Malyshev, J. Smiesko,
S. Tokar, *Eur. Phys.J. C* 79, 92 (2019)

S.J. Brodsky, G.I. Lykasov, A.V. Lipatov et al. / Progress in Particle and Nuclear Physics 114 (2020) 103802

23





^TThe $\mathcal{O}(\alpha\alpha_s)$ (a) and $\mathcal{O}(\alpha\alpha_s^2)$ (b) – (e) contributions to the $\gamma(Z) + Q$ production.

a)QCD compton; b),c) QQ annihilaton; d),e) flavour excitation

S.J.Brodsky, V.A.Bednyakov, G.L., J.Smiesko, S.Tokar, Progr.Part.Phys. v.93, 108 (2017)

S.J.Brodsky, G.L., A.V.Lipatov, J.Smiesko, Progr.Part.Phys. v.114, 103802 (2020)

PHOTON (DI-LEPTON) AND c(b)-JETS PRODUCTION IN P-P

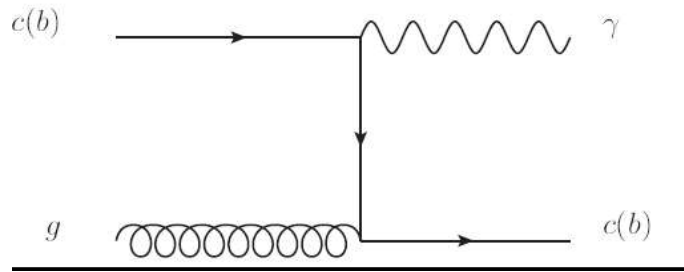


Fig.a. Feynman diagram for the process $c(b) + g \rightarrow \gamma + c(b)$

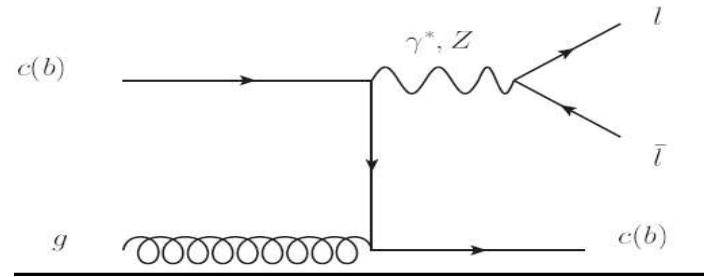


Fig.b. Feynman graph for the process $c(b) + g \rightarrow \gamma/Z^0 + c(b)$

$$x_F = \frac{2p_T}{S^{1/2}} sh(\eta); p_{T\gamma} = -p_{Tc} \quad x_{c(b)} = \frac{m^2}{x_g S} + x_{c(b)}^f$$

To observe the IC

for Fig.a

$$x_c \geq x_F > 0.1$$

for Fig.b

$$x_{c(b)} = \frac{m^2}{x_g S} + x_{c(b)}^f > 0.1$$

PRODUCTION OF HEAVY FLAVOURS IN HARD P-P COLLISIONS

$$E \frac{d\sigma}{d^3p} = \sum_{i,j} \int d^2k_{iT} \int d^2k_{jT} \int_{x_i^{\min}}^1 dx_i \int_{x_j^{\min}}^1 dx_j f_i(x_i, k_{iT}) f_j(x_j, k_{jT}) \frac{d\sigma_{ij}(\hat{s}, \hat{t})}{d\hat{t}} \frac{D_{i,j}^h(z_h)}{\pi z_h}$$

$$x_i^{\min} = \frac{x_T \cot(\frac{\theta}{2})}{2 - x_T \tan(\frac{\theta}{2})} \quad x_F \equiv \frac{2p_z}{\sqrt{s}} = \frac{2p_T}{\sqrt{s}} \frac{1}{\tan \theta} = \frac{2p_T}{\sqrt{s}} \sinh(\eta)$$

$$x_i^{\min} = \frac{x_R + x_F}{2 - (x_R - x_F)} \quad x_R = 2p/\sqrt{s}$$

One can see that $x_i \geq x_F$. If $x_F > 0.1$ then, $x_i > 0.1$ and the **conventional sea** heavy quark (extrinsic) contributions are suppressed in comparison to the **intrinsic** ones.

x_F is related to p_T and η . So, at certain values of these variables, in fact, there is **no conventional sea** heavy quark (**extrinsic**) contribution. And we can study the **IQ contributions** in hard processes at the **certain** kinematical region.